Baryon Form Factors at BESIII *

Yadi Wang[1)] (for BESIII Collaboration)

Helmholtz-Institut Mainz (GSI), Mainz 55128, Germany

Abstract: With the data collected by the BESIII detector at the BEPCII e^+e^- collider in 2013, we measured the cross section of $e^+e^- \to p\overline{p}$ at 12 center-of-mass energies from 2.2324 to 3.6710 GeV. The prospect of new results with the larger e^+e^- scanning data, collected in 2014 and 2015, is reported. The measurement of $p\overline{p}$ form factor with ISR has also been studied in both tagged and untagged methods. With the good performances of BESIII, the feasibility of $n\overline{n}$ form factors measurement in both ISR mode and scan mode is reported too. The preliminary but unexpected result of form factors of $\Lambda\overline{\Lambda}$ measurement is shown, as well as the expectation from the data collected at the threshold of $e^+e^- \to \Lambda_c\overline{\Lambda_c}$. We also expect from these data a measurement of form factors of all the other hyperons by BESIII.

Key words: Form factors, Baryons, Hyperons, BESIII

BESIII 上的重子形状因子

王雅迪（BESIII 合作组）

美因茨亥姆霍兹研究所，美因茨 55128，德国

摘要：利用在 2013 年，BEPCII 对撞机上的 BESIII 探测器收集的数据，我们测量了 $e^+e^- \to p\overline{p}$ 在 2.2324 到 3.6710GeV 之间 12 个质心系能量点的截面。我们期待利用在 2014 年和 2015 年收集的更大的 e^+e^- 扫描数据样本做更进一步测量。我们也通过标记和不标记初态辐射光子的方法，对 $p\overline{p}$ 形状因子进行了测量。利用 BESIII 的优良探测器表现，利用标记和不标记初态辐射光子的方法，我们对 $n\overline{n}$ 形状因子的测量进行了可行性研究。$\Lambda\overline{\Lambda}$ 的形状因子的初步但不符合理论预期的结果，及利用在 $e^+e^- \to \Lambda_c\overline{\Lambda_c}$ 阈值上收集的数据的预期也一并报道。我们也期望 BESIII 能对其他超子的形状因子进行测量。

关键词：形状因子，重子，超子，BES III

PACS: Ft., Ky

1 Introduction

The measurements of baryon form factors (FFs) in space-like region as well as in time-like region provide fundamental information on baryon structure, giving crucial tests also to models of hadron internal structure in general. Over its long history, the experimental results on FFs have driven and renewed models which are trying to explain FFs of Nucleons at low and high q^2, in space-like region as well as in time-like region. In a parity, time reversal and gauge invariant theory, the structure of any non-point-like particle of spin S is parametrized in terms of $(2S+1)$ FFs. Hence baryons with $\frac{1}{2}$ spin, which are considered here, are described by two electromagnetic FFs.

In the time-like (TL) region, assuming a metric where the momentum transfer squared q^2 is positive, the FFs have complex values, and their module can be measured by means of cross section and angular distribution measurement. By looking into the polarization of the outgoing baryons, the information on the relative phase can be achieved. The Sachs FFs, electric G_E and magnetic G_M, are introduced as linear combinations of the Dirac and Pauli FFs [1]. The Born cross section, that is the one virtual photon channel, is supposed to be the dominant one in the time-like region. That means the final states have the photon quantum numbers, in particular the same, negative, charge conjugation. As a consequence there should be a forward/backward symmetry. The two virtual photon would have the opposite one and the interference between these two contributions should produce a forward/backward asymmetry. Indeed a small asymmetry has been found in $e^+e^- \to \gamma_{ISR}p\overline{p}$ [8, 9]. Conversely, in the space-like region at high q^2) the very different behaviour of G_E and G_M has been assumed to be due to a strong contribution from the two photon exchange. The Born cross section can be written as a function of G_E and G_M, as in Eq. (1). The differential Born cross section can be written as in Eq. (2), by which the FFs ($|G_E|$

Received 29 Nov. 2015

∗ Supported by German Research Foundation DFG under Collaborative Research Center CRC-1044

1) E-mail: wangyd@ihep.ac.cn

and $|G_M|$ or $R = |\frac{G_E}{G_M}|$) can be measured.

$$\sigma_{Born} = \frac{4\pi\alpha^2\beta\mathcal{C}}{3q^2}\left[|G_M|^2 + \frac{1}{2\tau}|G_E|^2\right] \tag{1}$$

$$\frac{d\sigma_{Born}}{d\Omega} = \frac{\alpha^2\beta\mathcal{C}}{4q^2}\left[(1+\cos^2\theta)|G_M|^2 + \frac{1}{\tau}\sin^2\theta|G_E|^2\right] \tag{2}$$

The factor $\mathcal{C}$ is a correction to the Born cross section, due to Coulomb interaction between the outgoing charged baryons. Until now $\mathcal{C}$ has been supposed to be the same as for point-like fermions, because of the long range Coulomb interaction. Analiticity of the Dirac and Pauli FF requires $G_E(4M^2 = G_M(4M^2)$. However it might be that some of these assumptions (that have never been under discussion) have to be reviewed, as it seems according to the present data on baryon FFs. For this reason it is worthwhile to collect more data on this topic. BESIII is a detector on a e^+e^- collider with very good performances, that provides a good lab to measure the FFs of baryons.

2 Proton FFs

In the TL region, measurements of proton FFs have been performed by means of $e^+e^- \to p\overline{p}$ [2–6], by means of the radiative return $e^+e^- \to \gamma_{ISR}p\overline{p}$ [7–9], and also by means of $p\overline{p} \to e^+e^-$ [10–12]. While there are many, somewhat consistent, measurements concerning the total cross section, there are few, not consistent, data on the ratio $R = \frac{|G_E}{G_M|}$, mostly from BABAR [8] and PS170 [10].

Recently, based on 157 pb^{-1} collected at 12 scan points between 2.22 and 3.71 GeV in 2011 and 2012, proton FFs have been measured at BESIII [13]. The product of proton and anti-proton selection efficiency times initial-state-radiation (ISR) up to the next-to-leading (NLO) correction factor, $\epsilon(1+\delta)$, estimated by means of ConExc [14], is about 66% at 2.23 GeV, with a 15% reduction at 4 GeV. After ISR correction, cross section and effective FF are extracted according to Eq. (3) and Eq. (4). The cross section is shown in Fig. 1 (a). In Fig. 1 (b) R, as extracted from the angular distribution of the proton, is shown too. The method of moments (MM) (Eq. (5)) has also been used to evaluate R, see Table 1. The cross section has been measured with an accuracy between 6.0% and 18.9% up to $\sqrt{s} < 3.08$ GeV, improving the previous results and G_M has been measured too.

$$\sigma_{Born} = \frac{N_{obs} - N_{bkg}}{\mathcal{L}\epsilon(1+\delta)} \tag{3}$$

$$|G| = \sqrt{\sigma_{Born}}(1 + \frac{1}{2\tau})(\frac{4\pi\alpha^2\beta\mathcal{C}}{2E_{CM}^2}) \tag{4}$$

$$\langle\cos^2\theta_p\rangle = \frac{1}{N_{\rm norm}}\int \frac{2\pi\alpha^2\beta C}{4s}\cos^2\theta_p[(1+\cos^2\theta_p)|G_M|^2 + \frac{4m_p^2}{s}(1-\cos^2\theta_p)|R^2|G_M|^2]d\cos\theta_p. \tag{5}$$

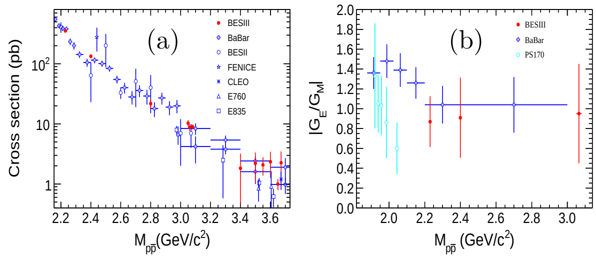

Fig. 1. The Born cross section (a) and R (b) from BESIII compared with other measurements.

Table 1. Results on R and G_M by fitting the proton angular distribution as well as by the method of moments at different c.m. energies.

$\sqrt{s}$ (MeV)	$\|G_E/G_M\|$	$\|G_M\|$ ($\times 10^{-2}$)
	Fit on $\cos\theta_p$	
2232.4	$0.87 \pm 0.24 \pm 0.05$	$18.42 \pm 5.09 \pm 0.98$
2400.0	$0.91 \pm 0.38 \pm 0.12$	$11.30 \pm 4.73 \pm 1.53$
(3050.0-3080.0)	$0.95 \pm 0.45 \pm 0.21$	$3.61 \pm 1.71 \pm 0.82$
	Method of moments	
2232.4	0.83 ± 0.24	18.60 ± 5.38
2400.0	0.85 ± 0.37	11.52 ± 5.01
(3050.0-3080.0)	0.88 ± 0.46	3.34 ± 1.72

At present, the precision of R is still dominated by statistics. In 2014 and 2015, BESIII has collected more data by means of an energy scan. These data will provide the opportunity to get better results on proton FFs.

The proton FFs has also been measured with the large XYZ dataset collected at BESIII by means of ISR technique, which allows a continuous q^2 measurement from the threshold. Detection efficiency depends slowly on q^2 and it is about 20% with γ_{ISR}-untagged mode, and about 6% with γ_{ISR}-tagged mode. Full angular distribution in hadronic center-of-mass is acquired, and the acceptance at threshold is non-zero, in the untagged mode. BESIII statistics is competitive with BABAR above $M(p\overline{p}) \sim 2.0$ GeV.

3 Neutron FFs

Up to now, the experimental results on neutron FFs are very few. Only FENICE [15] and SND [16] gave results about neutron effective FFs. This is due to the difficulties in detecting low energy n, when the n does not produce a hadronic shower yet in the electromagnetic calorimeter (EMC). The $\overline{n}$ annihilates and releases always a large amount of hadronic energy, more than twice the nucleon mass. The sources of background in detecting an $\overline{n}$ are other neutral particles, like γ, K_L^0 and mostly beam and neutral cosmic ray.

At BESIII, the depth of the EMC is about 15 photon radiation lengths, and about 50% of a hadronic interaction length, which is roughtly the probability of detecting high energy n and $\overline{n}$ interacting in the EMC. For a 1 GeV photon the EMC energy resolution is 2.5% in the barrel and 5.0% in the end-caps, which provides a chance to reconstruct at least the $\overline{n}$. The measurements can be performed by means of $e^+e^- \to n\overline{n}$ with the scanned data and by means of the radiative return $e^+e^- \to \gamma_{ISR} n\overline{n}$ using the XYZ data. The detection strategy could be: first identify $\overline{n}$ and γ_{ISR}; then the EMC shower information is used in those cases n identification is possible; finally event kinematics is used to further veto the remaining backcground. The EMC capability in distinguishing between $\overline{n}$ and photon is comprehensively studied with the Toolkit for Multivariate Data Analysis in the ROOT (TMVA) package. The result is shown in Fig. 2, where one can see that $\overline{n}$ and photon are well seperated.

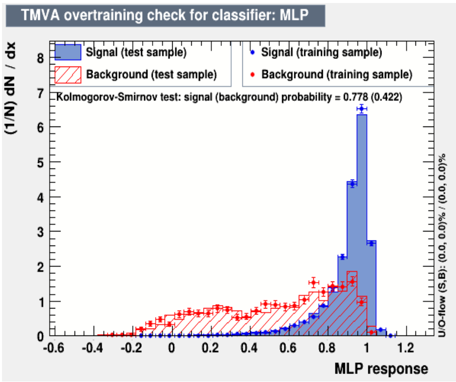

Fig. 2. The EMC capability in distinguishing between $\overline{n}$ and photon studied with TMVA package. The hatched histogram and dots are for signal. The other histogram and dots are for background from a photon.

To increase the overall detection efficiency, relaxing n identification, the muon counter (MUC) and the TOF counters can be exploited. MUC is made of Resistive Plate Counters interleaved with the yoke iron. The yoke iron is about 54 cm in total, which makes $\sim 96\%$ the probability the $\overline{n}$ interacts in MUC. TOF counters are fired by the $\overline{n}$ annihilation star and the TOF measurement might be enough to get rid of n detection. So these are additional possibilities to detect $\overline{n}$ at BESIII, and their feasibility is under study.

4 Λ FFs

The Coulomb factor should not enter the cross section formula in the case of a neutral baryon pair. Therefore the Born cross section is expected to vanish at threshold, increasing with the velocity of baryon. The $\Lambda\overline{\Lambda}$ cross section and FFs have been measured by BABAR by means of ISR technique, from threshold to 2.27 GeV, with a non-zero cross section of $(204 \pm 60 \pm 20)$ *pb*. This result may conflict with the theory prediction but it is integrated on a large energy interval, because of ISR.

With the data collected in 2012, the FFs of $\Lambda\overline{\Lambda}$ has been measured at BESIII preliminarily at four energy points, 2232.4, 2400.0, 2800.0, 3080.0 MeV and a search has been done by looking at $\Lambda \to p\pi^-$ and $\Lambda \to n\pi^0$. At 2232.4 MeV, very close to the threshold, the momentum of final proton is too low to leave message in the detector and the antiproton interacts on the beam pipe. However it is possible to exploit the fact that in the $\Lambda \to \overline{p}\pi^0$ decaying vertex of the secondary particles produced by $\overline{p}$ in the beam pipe is 3 cm displaced, due to the interaction with the beam pipe. For $\Lambda \to n\pi^0$ selection, the TMVA based on Boosted Decision Tree is applied to veto large background. The π^0 in the final state has a monochromatic momentum, about 105 MeV. According to the aforementioned features, 43 ± 7 events have been selected from $\Lambda \to \overline{p}\pi^0$ mode, and 22 ± 6 events from $\Lambda \to n\pi^0$ mode. Surprisingly, a large cross section, about 320 ± 58 *pb* very close (~ 1 MeV above) to the threshold has been observed. Cross section and effective FF are listed in Table 2. Figure 3 shows $\Lambda\overline{\Lambda}$ cross section, as measured by BESIII, BABAR [17] and DM2 [18].

Table 2. BESIII results on $\Lambda\overline{\Lambda}$ cross section and effective form factor.

$\sqrt{s}$ (MeV)	σ_{Born} (pb)	$\lvert G\rvert$ $(\times 10^{-2})$
2232.4		
$\Lambda \to p\pi^-, \overline{\Lambda} \to \overline{p}\pi^+$	$325 \pm 53 \pm 46$	
$\overline{\Lambda} \to \overline{n}\pi^0$	$(3.0 \pm 1.0 \pm 0.4) \times 10^2$	
combined	320 ± 58	63.4 ± 5.7
2400.0	$133 \pm 20 \pm 19$	$12.93 \pm 0.97 \pm 0.92$
2800.0	$15.3 \pm 5.4 \pm 2.0$	$4.16 \pm 0.73 \pm 0.27$
3080.0	$3.9 \pm 1.1 \pm 0.5$	$2.21 \pm 0.31 \pm 0.14$

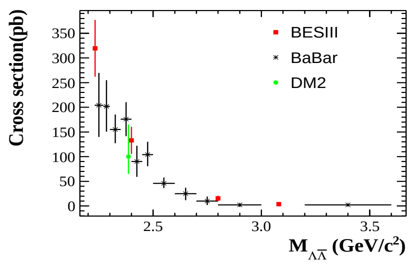

Fig. 3. BESIII, BABAR and DM2 measurements of $\Lambda\overline{\Lambda}$ from 2.0 up to 3.6 GeV.

Due to parity violating decay of $\Lambda \to p\pi$, the proton emission depends on Λ polarization in the $\Lambda\overline{\Lambda}$ frame. The imaginary part of FFs leads to a polarization observable, as shown in Eq. (6). θ_Λ is the polar angle of Λ

in $\Lambda\overline{\Lambda}$ frame. θ_p is the polar angle of p in Λ frame. According to the data taken in 2014 and 2015, a statistical accurancy between 6% and 17% for P_n can be achieved.

$$P_n = -\frac{\sin 2\theta \sin\Delta\phi/\tau}{R\sin^2\theta_\Lambda \tau + (1+\cos^2\theta_\Lambda^2)/R} = \frac{3}{\alpha_\Lambda} < \cos\theta_p > \quad (6)$$

5 FFs of Λ_c and other hyperons

The Coulomb enhancement factor $\mathcal{C}$ at threshold, in the case of $e^+e^- \to \Lambda_c\overline{\Lambda_c}$ predicts $\sigma_{Born} = \frac{\pi^2\alpha^3}{2M^2}|G|^2 = 0.15|G|^2$ nb. Results from Belle [19] indicate that the cross section near the threshold of $\Lambda_c\overline{\Lambda_c}$ is nearly 0.15 nb, which means $G \sim 1$ at threshold. This strange result is consistent with what has been found by BABAR in $e^+e^- \to p\overline{p}$. Also the ratio R, as measured by BABAR, might be unexpected, being different from 1 (but integrated on an energy interval) as expected according to analiticity. However, the Belle result is affected by a very large error. To verify this, more integrated luminosity is needed. BESIII collected at 4575 MeV, very close to the threshold, an integrated luminosity of 42 pb^{-1}. Very likely, BESIII will collect more data at high energy. Thus, the cross section measurement will be largely improved, and a 10% precision in the measurement of R is expected with a luminosity of 200 pb^{-1}, assuming an R value similar to the one found in the proton case at BABAR.

Taking the advantage of the large energy range and large data samples at BESIII, the TL-FFs of other hyperons, such as $\Lambda\overline{\Sigma^0}$, $\overline{\Sigma^0}\Sigma^0$, $\overline{\Sigma^-}\Sigma^+$, $\overline{\Sigma^+}\Sigma^-$, $\overline{\Xi^0}\Xi^0$, $\overline{\Xi^+}\Xi^-$, $\overline{\Omega^+}\Omega^-$, together with the measurements of R and relative phase $\Delta\Phi$ at single energy points will be extracted.

6 Summary

BESIII is an excellent laboratory for baryon form factor measurements. Both scan and ISR techniques can be used. The proton FFs and the ratio have been measured using 2013 data. With the same data, preliminary results on $\Lambda\overline{\Lambda}$ have been just released. With higher statistics between 2.0 and 3.1 GeV, collected in 2014 and 2015, new significant results will come and improve FFs status for p, n, Λ, Ξ, Ω, Σ, Λ_c. Also the measurements with XYZ datasets by ISR method is worth anticipating.

References

1 F.Halzen, A. D. Martin, Quarks and Leptons: An Introductory Course in Modern Particle Physics, Canada, John Wiley&Sons, 1984:172.
2 B.Delcourt *et al.* (DM1 collaboration), Phys. Lett. B 86 (1982) 395.
3 D. Bisello *et al.* (DM2 Collaboration), Nucl. Phys. B224 (1983) 379; Z. Phys. C 48 (1990) 23.
4 A. Antonelli *et al.* (FENICE Collaboration), Nucl. Phys. B517 (1998) 3.
5 M. Ablikim *et al.* (BES Collaboration), Phys. Lett. B 630 (2005) 14.
6 T. K. Pedlar *et al.* (CLEO Collaboration), Phys. Rev. Lett. 95 (2005) 261803.
7 J. P. Lees *et al.* (BABAR Collaboration), Phys. Rev. D 73 (2006) 012005.
8 J. P. Lees *et al.* (BABAR Collaboration), Phys. Rev. D 87 (2013) 092005.
9 J. P. Lees *et al.* (BABAR Collaboration), Phys. Rev. D 88 (2013) 072009.
10 G. Bardin *et al.* (PS170 Collaboration), Nucl. Phys. B411 (1994) 3.
11 T. A. Armstrong *et al.* (E760 Collaboration), Phys. Rev. Lett. 70 (1993) 1212.
12 M. Ambrogiani *et al.* (E835 Collaboration), Phys. Rev. D 60 (1999) 032002; M. Andreotti *et al.*, Phys. Lett. B 559 (2003) 20.
13 M. Ablikim *et al.* (BESIII Collaboration), Phys. Rev. D 91 (2015) 112004.
14 R. G. Ping, Chin. Phys. C 38 (2014) 083001.
15 A. Antonelli *et al.* (FENICE Collaboration), Nucl. Phys. B 517 (1998) 3.
16 M. N. Achasov *et al.* (SND Collaboration), Phys. Rev. D 90 (2014) 112007.
17 B. Aubert *et al.* (BaBar Collaboration), Phys. Rev. D 76 (2007) 092006.
18 D. Bisello *et al.* (DM2 Collaboration), Z. Phys. C 48 (1990) 23.
19 G. Pakhlova *et al.* (BELLE Collaboration), Phys. Rev. Lett. 101 (2008) 172001.